Clustering in real space and in redshift space

Nick Kaiser *Institute of Astronomy, University of Cambridge, Madingley Road, Cambridge CB3 0HA*

Summary. Peculiar velocities distort the clustering pattern in redshift space on all scales. Four consequences of this are:

(i) The acceleration vector derived by summing the inverse squared redshifts of galaxies differs significantly from the true acceleration even in linear theory. Estimates of Ω obtained in this manner are only reliable for small Ω.

(ii) The power spectrum of large-scale clustering has a quadrupole anisotropy, providing a way to estimate Ω. We calculated, for various assumed power spectra, the line-of-sight correlation function in redshift space, ξ_v. We find that ξ_v may display a strong anticorrelation feature that has no counterpart in real space.

(iii) The density contrast of the local supercluster will appear enhanced in redshift space. Using a simple infall model (with $\Omega=1$), we simulate the Shapley–Ames catalogue. For an infall velocity around $350\,\mathrm{km\,s^{-1}}$, the apparent density is similar to that observed, so the data do not require $\Omega \ll 1$, or biasing on large scales.

(iv) Turnaround is estimated to occur at a radius $\simeq 1500\,\mathrm{km\,s^{-1}}$ from a rich cluster, resulting in large transverse features of this scale. Since the velocity field is apparently very coherent, high density caustic surfaces must result. Guided by the appearance of the spherical model, we argue that the shell-like structures seen in some recent redshift surveys are most naturally interpreted as these caustics, rather than as the result of energetic explosions. The model also shows the apparent falling velocity dispersion with radius that is often seen in rich clusters, and suggests that the interpretation of this in terms of equilibrium models is inappropriate.

1 Introduction

Several extensive galaxy redshift surveys are now available, and these provide a reasonably precise three-dimensional view of the world. In a perfectly homogeneous Friedmann universe these redshifts would accurately measure radial distance from the observer, and the mapping from real space (*r*-space) to redshift space (*s*-space) would simply be an identity. In an inhomogeneous universe like our own the peculiar velocities associated with any inhomogeneous

structure will introduce a distortion in this mapping. In this paper we will explore several aspects of this distortion.

Perhaps the most obvious example of this distortion is the 'finger of God' effect which causes the dense central regions of clusters of galaxies to appear elongated along the line-of-sight. Inside a virialized cluster the velocity of a particle is essentially uncorrelated with its position, and the resulting distribution of galaxies in redshift space is just the convolution of the distribution in real space with the distribution of velocities. If we try to measure galaxy clustering on larger scales from redshift surveys, it is probably reasonable to model the effect of clustering on smaller scales by a similar position-independent distribution function, with a width of a few hundred km s^{-1}. Presumably with this type of *incoherent* velocity field in mind, it has been asserted that on large scales, where the separation is much greater than the typical random velocities, the effect of peculiar velocities on clustering statistics such as the two-point correlation function $\xi(r)$ can be neglected (e.g. Kirshner, Oemler & Schechter 1979; Davis & Peebles 1983; Shanks *et al.* 1983). It is not difficult to see, however, that the *coherent* velocity fields associated with any large-scale structure will significantly distort the clustering pattern even on very large scales.

The simplest example which displays this distortion is the simple 'top-hat' homogeneous sphere perturbation: if the background universe has Hubble ratio, H, and the perturbation has a small fractional density enhancement $\Delta\varrho/\varrho$, the fractional perturbation to the Hubble ratio is $\Delta H/H = -(1/3)f(\Omega)\,\Delta\varrho/\varrho$, with $f(\Omega) = \Omega^{0.6}$ to a good approximation. For an observer outside the perturbation, the overdense region will appear in redshift space to be slightly squashed along the line-of-sight by an amount $\Delta H/H$, and the apparent overdensity will be greater than the true value by the factor $[1+f(\Omega)/3]$. In a universe with $\Omega=1$, and containing such perturbations, the correlation function measured in redshift space, ξ_s, which essentially measures the square of the density enhancement for linear perturbations, would therefore be expected to be roughly 16/9 times larger than the true correlation function. While this simple model is highly idealized, it reveals two features of the redshift space distortion which are quite general: first, since the effect (at least for growing perturbations) is to shrink overdense regions and inflate underdense regions, the amplitude of the clustering will typically be enhanced. Secondly, in contrast to the elongation along the line-of-sight produced by incoherent velocity fields, the clustering pattern will appear compressed along the line-of-sight.

It would, of course, be desirable to be able to invert the distortion process to obtain, from estimates of clustering in redshift space, the true spatial distribution. In general this is quite a difficult problem, but there are various applications of redshift surveys where some progress can be made, either by constructing models or by making simplifying assumptions. In this paper four such applications will be considered.

In the following section we consider the problem of estimating the acceleration vector from a magnitude-limited redshift survey. This quantity has been estimated from the revised Shapley–Ames (RSA) catalogue by Yahil, Sandage & Tammann (1980), hereafter YST, and from the Center for Astrophysics (CfA) redshift survey by Davis & Huchra (1982), hereafter DH. The motivation for these estimates is that they provide an appealingly simple way to estimate Ω. If one assumes that the major part of our velocity with respect to the cosmic frame defined by the microwave background is induced by fluctuations on rather large scales, and that these are adequately described by linear theory, then a simple linear relationship between the acceleration vector and this peculiar velocity should exist. For a magnitude-limited redshift survey the acceleration vector can be expressed as the vector sum over all the galaxies of a distance-dependent weight function divided by the square of the radial distance. The weight function is necessary because, for a magnitude-limited survey, a given number of galaxies nearby is indicative of a smaller amount of mass than the same number found at a greater distance. The approach that has previously been adopted is simply to substitute redshift for radial distance in

this sum. If Ω is not very small then the estimate of the acceleration vector performed in redshift space differs from the true value by correction terms which we calculate (to first order in the perturbation amplitude), and which we show to be typically larger than the true acceleration vector. This result is rather unfortunate since although the assumption that galaxies fairly trace the mass distribution on the very large scales of interest here is not entirely compelling, it is at least not obviously false. We conclude that, without very detailed modelling of the space distribution of galaxies, these estimates of the acceleration vector do not allow one to usefully contain the value of Ω.

In Section 3 we consider the anisotropy of the galaxy clustering pattern. As in Section 2 we restrict attention to large scales for which linear theory should be applicable, and assume that galaxies fairly trace the mass on these scales. We further restrict attention to fairly deep surveys wherein there is a useful volume of space in which the weight function is slowly varying on the scales of interest. Peebles (1980, section 76) has given expressions for the two-point galaxy correlation function based on an approximate model for the streaming motion; here we solve for the anisotropy of the power spectrum of galaxy clustering exactly (subject to the assumption of linearity). The relation between the power spectra in real and redshift space is very simply stated, but since few estimates of this quantity have been made, it is of more practical use to consider the correlation function. We calculate the direction averaged two-point function in redshift space and find that this differs from the real space correlation function only by an Ω dependent factor, so this provides one with a useful method to estimate Ω. We also consider the two-point function restricted to separations along the line-of-sight, ξ_v, as obtained from 'pencil-beam' redshift surveys (e.g. Shanks *et al.* 1983; Kirshner *et al.* 1979), or from estimates of clustering of QSO absorption features (Sargent *et al.* 1980; Webb 1986, in preparation). We calculate ξ_v for an assumed power law $\xi_r(r)$ and from this we draw some general conclusions, we find in particular that strong features like the anticorrelation feature suggested by the Durham survey can easily arise without any similar feature in true correlation function. Also, we show that for a particular power law form for $\xi_r(r)$, the line-of-sight correlation function in redshift space vanishes, a result which may be relevant to the interpretation of the absence of clustering of Lyman-α absorption systems.

In Section 4 we shift attention to another important application of redshift surveys, but one for which linear theory is probably not a very good approximation. This is the problem of determining the density parameter from our infall to the local supercluster. The density of the LSC has been estimated using both the RSA and CfA catalogues. While the CfA catalogue has the advantage of greater depth, it has the disadvantage that the sky coverage cuts off quite close to the Virgo cluster and consequently only a part of the supercluster is sampled. The RSA catalogue has much better sky coverage and is arguably the best available sample, for this purpose. YST estimate that the overdensity of the supercluster within our radius is $\sim$3, and combining this with the estimates of our infall velocity in the simple non-linear spherical collapse model results in $\Omega \simeq 0.05$. There is, however, one unsettling feature of the analysis of YST: they made no allowance for peculiar velocities in determining the density contrast and this raises the question as to whether the density contrast may have been overestimated. The situation in the literature regarding the importance of the correction for peculiar velocities is somewhat confusing: DH argued that the correction was important and, if not applied would lead to a significant underestimate of Ω. Yahil (1981) argued that the correction was very slight, thus vindicating the neglect of this in the earlier paper, and that if the correction was applied to the RSA analysis this would actually result in a slight *decrease* in the inferred value of Ω. In an attempt to explore this point further we have constructed what is perhaps the simplest model which incorporates the relevant features. We have laid down a simple spherical structure with a density contrast which falls off as r^{-2}, and which resides in a marginally closed background universe. We have populated

this with galaxies drawn from a realistic luminosity function and from this we have constructed a magnitude-limited sample with sky coverage like that of the RSA catalogue. This model is specified by two parameters: our peculiar velocity towards the centre of the enhancement and the recession velocity. It is quite easy to find acceptable values for these parameters for which the overall appearance of the cluster in redshift space is very similar to that observed (even though the true density contrast is only about 80 per cent, the apparent overdensity is much greater), and when we calculate the density field in the manner of YST we find good agreement. We conclude that, unless the estimates of our infall velocity are revised drastically downwards, the observations do not exclude a value of $\Omega \simeq 1$.

In Section 5 we consider the influence of peculiar velocities on the morphology of clustering in the transition between the linear and non-linear regimes. As we have already discussed in Section 3, small-amplitude clustering on large scales will appear compressed along the line-of-sight. As one approaches the non-linear clustering regime, this compression will become much more pronounced, with regions which are just turning around being crushed completely flat in redshift space. Using the cluster–galaxy cross-correlation function to estimate the typical profile around a rich cluster, we show that one can expect these to be associated with predominantly transverse artefacts in redshift space which extend to great distances from the clusters, and which contain roughly an order of magnitude more galaxies than partake of the better appreciated 'finger of God' artefacts. We suggest that these distortions are well able to account for the scale and general appearance of the connected features which are seen in the surveys of Giovanelli & Haynes (1985), Giovanelli, Haynes & Chincarini (1986), and in the survey by de Lapparent, Geller & Huchra (1986). The spherical model displayed here also sheds some light on the falling velocity dispersions commonly seen in rich clusters (e.g. Kent & Gunn 1982; Kent & Sargent 1983). These are usually interpreted in the framework of equilibrium models. The models considered here have a very similar appearance, and suggest a different interpretation.

The ordering of these four sections is thus: linear density fluctuations in our vicinity (Section 2); linear density fluctuations at large distances (Section 3); non-linear fluctuations in our vicinity (Section 4); and non-linear clustering at greater distances (Section 5). In Section 6 we discuss the interpretation of the quantity Ω that may be obtained from the methods of Sections 3 and 4, in the context of 'biased' theories for galaxy formation in which the assumption that galaxies fairly trace the mass is invalid.

2 The acceleration vector

The local group has a velocity of $\simeq 600\,\mathrm{km\,s^{-1}}$ relative to the microwave background, in a direction about 45° away from the Virgo cluster. Our infall with respect to the local supercluster accounts for only a small fraction of this, and it is usually assumed that the bulk of this velocity is induced by the gravitational pull of more distant regions. Since this velocity is considerably less than the Hubble velocity across the scale of the region which is assumed to be accelerating towards us, linear theory should provide a valid description.

If we define

$$\mathbf{a}_r \equiv \int_{V_r} d^3r\, \Delta(\mathbf{r})\, \frac{\mathbf{r}}{r^3} \tag{2.1}$$

where $\Delta(\mathbf{r})$ is the density contrast and V_r is the survey volume, then, in linear theory, the peculiar velocity of the particle at the origin is

$$\mathbf{v} = \frac{2}{3} \frac{G\varrho_{\mathrm{crit}}\mathbf{a}}{H} f(\Omega) \tag{2.2}$$

with $f(\Omega)\simeq\Omega^{0.6}$. If one had distances r to all galaxies in a magnitude-limited catalogue, one could estimate $\mathbf{a}_r$ as

$$\mathbf{a}_r=\langle n_r(\mathbf{r})/\phi(r)\rangle^{-1}\int_{V_r}d^3r\ \frac{\mathbf{r}}{r^3}\ \frac{n_r(\mathbf{r})}{\phi(r)},\tag{2.3}$$

where $n_r(\mathbf{r})\,d^3r$ is the number of galaxies counted in a volume element d^3r around $\mathbf{r}$, and $\phi(r)$ is the selection function:

$$\phi(r)=\int_{L_{\text{limit}}}^{\infty}\Phi(L)\ dL,$$

where $\Phi(L)$ is the luminosity function, and L_{limit} is the absolute luminosity of a galaxy which just enters the catalogue at distance r. We have assumed here for simplicity that the survey volume has

$$\int_{V_r}d^3r\ \frac{\mathbf{r}}{r^3}=0,$$

so we were able to replace $\Delta(\mathbf{r})$ in equation (2.1) by the estimate of

$$1+\Delta(\mathbf{r})=[n_r(\mathbf{r})/\phi(r)]\times\text{constant}.$$

We have also assumed that the probability of finding a galaxy of a given type in a given volume is just proportional to the amount of matter in that volume, i.e. that galaxies are drawn from a universal luminosity function and their distribution in space fairly reflects the mass distribution.

With this estimate of $\mathbf{a}_r$ we would be able to estimate Ω through equation 2.2. In practice we do not have positions for the galaxies, we have instead the coordinates $\mathbf{s}$ in redshift space. The approach that has been adopted in the past is simply to replace real distances by redshifts in equation 2.3 (YST, DH). We shall now show that, unless Ω is very small compared to unity, this quantity (which we shall denote by $\mathbf{a}_s$) is unlikely to be even approximately equal to the desired acceleration vector $\mathbf{a}_r$.

Given the peculiar velocity field $\mathbf{v}(\mathbf{r})$, we can define the line-of-sight component:

$$U(r)\equiv\mathbf{v}(\mathbf{r})\cdot\hat{\mathbf{r}}\tag{2.4}$$

where $\hat{\mathbf{r}}$ is a unit vector.

The mapping from r-space to s-space is then

$$\mathbf{s}(\mathbf{r})=\mathbf{r}\left[1+\frac{U(\mathbf{r})-U(0)}{r}\right],\tag{2.5}$$

where we have chosen units such that $H=1$. The Jacobian of this transformation is

$$d^3s=d^3r\left[1+\frac{U(\mathbf{r})-U(0)}{r}\right]^2\left[1+\frac{dU(\mathbf{r})}{dr}\right].\tag{2.6}$$

Now $n_s(\mathbf{s})\,d^3s=n_r(\mathbf{r})\,d^3r$ by definition, so we have

$$\begin{aligned}\mathbf{a}_s&\equiv\left\langle\frac{n_s(\mathbf{s})}{\phi(s)}\right\rangle^{-1}\int_{V_s}d^3s\ \frac{\mathbf{s}}{s^3}\ \frac{n_s(\mathbf{s})}{\phi(s)}\\&=\frac{\langle n_r(\mathbf{r})/\phi(r)\rangle}{\langle n_s(\mathbf{s})/\phi(s)\rangle}\int_{V_s}d^3r\ \frac{\mathbf{r}}{r^3}\left[1+\frac{U(\mathbf{r})-U(0)}{r}\right]^{-2}\frac{\phi(r)}{\phi[s(r)]}\ \frac{n_r(\mathbf{r})/\phi(r)}{\langle n_r(\mathbf{r})/\phi(r)\rangle}.\end{aligned}\tag{2.7}$$

If we calculate only to first order in the perturbation, the factor preceding the integral can be

replaced by unity, since the integral itself is of first order in the perturbation amplitude. The relation between $\mathbf{a}_s$ and $\mathbf{a}_r$ is most clearly seen for the case of a spherical survey volume V_s in s-space. Performing the usual decomposition into independent plane waves:

$$\Delta(\mathbf{r}) = \sum \Delta(\mathbf{k}) \cos(\mathbf{k} \cdot \mathbf{r} + \theta_{\mathbf{k}}),$$

we can consider each mode separately and combine the results at the end of the day. For the perturbation

$$\Delta(\mathbf{r}) = \Delta_0 \cos(\mathbf{k} \cdot \mathbf{r} + \theta)$$

we have

$$\mathbf{v}(\mathbf{r}) = -\frac{\mathbf{k}}{k^2} \Omega^{0.6} \Delta_0 \sin(\mathbf{k} \cdot \mathbf{r} + \theta).$$

Since the survey volume is isotropic we can take the wave-vector, $\mathbf{k}$, to lie along the z-axis for convenience.

In order to reduce equation (2.7) to a reasonably simple form let us finally make the assumption that the survey is deeper than the scale of the perturbation, so that the survey volume fully encloses the source of our peculiar motion. This is not very restrictive since, in order for the method to work at all it is necessary to make this assumption. Mathematically, this corresponds to taking the limit $kr_{max} \gg 1$, where r_{max} is the depth of the survey.

We then have

$$a_r = -4\pi \frac{\Delta_0}{k} \sin(\theta)$$

and

$$a_s = a_r + \Omega^{0.6} \left\{ \frac{a_r}{3} + 2\pi \frac{\Delta_0}{k} \int_{-1}^{+1} \mu^2 \, d\mu \int_0^{r_{max}} \frac{dr}{r} \left(2 + \frac{d \ln \phi}{d \ln r} \right) [\sin(\mu kr + \theta) - \sin \theta] \right\}. \tag{2.8}$$

We can see from this that, for $\Omega \to 0$, in which case peculiar velocities become negligible, we have $a_s \to a_r$ as expected. For $\Omega \neq 0$, the terms in brackets are the correction terms due to these velocities. The first of these is a 'surface term' which arises because the sphere of integration, which is concentric about the observer in s-space, maps to a displaced sphere in r-space. The term is relatively harmless since it simply gives rise to a multiplicative factor $(1 + \Omega^{0.6}/3)$, which can easily be corrected for. It is the second term which is more problematic. The magnitude of this term can be estimated as follows: for $r \gg k^{-1}$, the first sinusoid in equation (2.8) oscillates rapidly, and the contribution to the integral cancels out. The second (constant) sine factor, on the other hand, gives a logarithmically divergent contribution. This log divergence is cut-off at large r by the depth of the survey, and for $r \ll k^{-1}$ the two sine terms cancel, and this cuts off the divergence at small r. The result is

$$a_s - a_r \sim \Omega^{0.6} a_r \ln[(kr_{max})^2 \phi(r_{max})/\phi(k^{-1})]. \tag{2.9}$$

This is typically larger than the desired term a_r by an appreciable logarithmic factor. The problem is not alleviated by correcting for the observer's peculiar velocity, as for instance in DH. Such a correction only results in another logarithmically divergent contribution to a_s due to galaxies close to the observer. In practice this divergence will be cut-off by the finite number density of nearby galaxies, but in an unpredictable manner.

The presence of this k-dependent correction to a_s presents a severe problem which undermines

this method for determining Ω. In order to predict even the sign of this term requires knowledge of which region of space is dominating our peculiar acceleration, and in order to evaluate this correction with any degree of precision, one would need to construct an elaborate model for the density and velocity fields and then fit this to the data. While this would be possible in principle, it is a far cry from the simple, model-independent technique as originally presented. It should be clear then that the estimates of $\mathbf{a}_s$ that have been extracted from magnitude-limited redshift surveys do not usefully constrain the value of Ω. This is unfortunate, since the assumption that galaxies fairly trace the mass on the very large scales relevant for this problem is, if not entirely compelling, at least an interesting and natural hypothesis, and the proposed method has the great appeal of simplicity. We shall show in the next section that there is an alternative test for Ω which, while it is somewhat more demanding in the data required for its execution, makes just the same assumptions as the method we have discussed above, but does not suffer from the same problems.

3 Anisotropy of galaxy clustering

In the previous section we were concerned with density fluctuations in our vicinity which are presumed to be responsible for our peculiar velocity. We found that the estimator of the density, when applied in redshift space, was significantly perturbed by the peculiar velocities. If we compare the estimate of the density in a small volume element of redshift space with the true density, we can identify three effects due to peculiar velocities. First, each point in the volume element will be translated radially, by an amount $\Delta r = U(\mathbf{r}) - U(\mathbf{0})$, and so the volume will undergo a fractional change $2\Delta r/r$. Secondly, the selection function will change by a fraction $(d \ln \phi/d \ln r) \Delta r/r$. Thirdly, if there is any shear in the velocity field this volume element will be stretched or compressed. For perturbations in our vicinity all of these terms are appreciable, and it is for this reason that it is so difficult to invert the combined effect of these distortions. For density fluctuations at great distance from us there will also be significant distortions, but the first two of the terms we have identified become negligible, since the radial displacements become parallel at large r and the selection function will become very slowly varying on the scale of the perturbation, so only the effect of the shear will remain. In this section we shall show that, in the appropriate limit, it is possible to invert the distortion for linear perturbations. The inversion is very simple, at least when expressed in Fourier space where it shows up as simple quadrupole angular dependence. If one makes the natural assumption that the clustering pattern in real space is statistically isotropic, then Ω can be estimated by measuring the anisotropy of the power spectrum in s-space. Since few estimates of the power spectrum are available it is of more practical use to consider the anisotropy of the correlation function. This turns out to be somewhat more complicated, but some progress can be made. We give particular attention to two problems. First, we calculate the amplitude of the correlation function when direction averaged in redshift space. This gives a reasonable approximation to the estimates of $\xi(s)$ that have been extracted from the CfA survey, and other surveys with a large solid volume. Secondly, we explore the relation between ξ_s and ξ_r when the separations are restricted to lie along the line-of-sight. This is appropriate for large separations in 'pencil beam' redshift surveys and also for the clustering of QSO absorption systems.

3.1 THE POWER SPECTRUM

Recall that, for the magnitude-limited survey, the estimate of the density in real space is, up to a constant, given by

$$\varrho_r(\mathbf{r}) = n_r(\mathbf{r})/\phi(r). \tag{3.1}$$

The corresponding quantity in redshift space: $\varrho_s(\mathbf{s}) = n_s(\mathbf{s})/\phi(s)$ is related to ϱ_r via the transformation (2.5) and its Jacobian (2.6), as

$$\varrho_s(\mathbf{r}) = \frac{\phi(r)}{\phi\{r[1+(U(r)-U(0))/r]\}} \left[1 + \frac{U(r)-U(0)}{r}\right]^{-2} \left(1 + \frac{dU}{dr}\right)^{-1} \varrho_r(\mathbf{r}), \qquad (3.2)$$

so, to first order in the perturbation, we have

$$\Delta_s(\mathbf{r}) = \Delta_r(\mathbf{r}) - \left(2 + \frac{d\ln\phi}{d\ln r}\right)\left[\frac{U(r)-U(0)}{r}\right] - \frac{dU}{dr}. \qquad (3.3)$$

For a plane-wave density ripple $U \sim \Delta/k$ and $dU/dr \sim kU \sim \Delta$. For a survey of depth $r_{max} \gg k^{-1}$, the second term in equation (3.3) becomes negligible compared to Δ except very near to the observer but the third term due to the shear of the velocity field remains of the same order as Δ and therefore must be retained. For the Fourier mode

$$\Delta_r(\mathbf{r}) = \Delta_{\mathbf{k}} \cos(\mathbf{k}\cdot\mathbf{r} + \theta),$$

we have

$$U(\mathbf{r}) = -\frac{\mu\Omega^{0.6}\Delta_{\mathbf{k}}}{k} \sin(\mathbf{k}\cdot\mathbf{r} + \theta),$$

where μ is the cosine of the angle between $\mathbf{k}$ and the line-of-sight, and therefore

$$\frac{dU}{dr} = -(\mu^2\Omega^{0.6}\Delta_{\mathbf{k}})\cos(\mathbf{k}\cdot\mathbf{r} + \theta)$$

$$= -\mu^2\Omega^{0.6}\Delta_r(\mathbf{r}),$$

so

$$\Delta_s(\mathbf{r}) = \Delta_r(\mathbf{r})(1 + \mu^2\Omega^{0.6}). \qquad (3.4)$$

We see from this that a plane-wave density ripple in r-space maps to a plane-wave density ripple in s-space with the same phase and wave-vector but with enhanced amplitude. The relation between the power spectra $P(\mathbf{k}) \equiv \langle |\Delta_{\mathbf{k}}|^2 \rangle$ in r-space and s-space.

$$P_s(\mathbf{k}) = P_r(\mathbf{k})(1 + \Omega^{0.6}\mu^2)^2. \qquad (3.5)$$

So, if $\Omega = 1$ for instance, and the power spectrum in real space is isotropic, the power measured in s-space varies considerably with angle, being four times larger for wave-vectors parallel to the line-of-sight than for transverse wave vectors.

Equation (3.5) therefore provides a way to estimate Ω. Simply estimate the power spectrum in s-space for various directions $\hat{\mathbf{k}}$, and then fit to the predicted μ-dependence to find Ω. However, since the power spectrum will probably be estimated as the Fourier transform of the correlation function, and estimates for ξ are already available, it is of more practical use to find a way to determine Ω directly from the correlation function. The rest of this section will therefore be devoted to exploring the anisotropy of the correlation function in s-space.

3.2 THE DIRECTION AVERAGED CORRELATION FUNCTION

The correlation function $\xi(\mathbf{r})$ is the Fourier transform of the power spectrum

$$\xi(\mathbf{r}) = \int d^3k P(\mathbf{k}) \exp(i\mathbf{k}\cdot\mathbf{r}), \qquad (3.6)$$

and this quantity can be conveniently estimated from redshift surveys, the estimator of $1+\xi(\mathbf{x})$ being the number of pairs with separation $\mathbf{x}$ divided by the number of pairs that one would obtain for a Poissonian distribution of points with the same selection function.

The correlation function in real space, ξ_r, is isotropic, and is given by

$$\xi_r(r)=4\pi\int_0^\infty dk\,k^2 P_r(k)\,\frac{\sin(kr)}{kr}. \tag{3.7}$$

The correlation function in s-space will be function of both s and μ, the cosine of the angle between the separation, $\mathbf{s}$, and the line-of-sight. Unlike the power spectrum though, where the anisotropy has the simple form of equation (3.5), the angular dependence of ξ can be quite complicated. It is, however, fairly straightforward to calculate the direction averaged correlation function in redshift space. The result is

$$\xi_{\langle s\rangle}(s)\equiv(1/2)\int_{-1}^{+1}d\mu\,\xi_s(s,\mu)$$

$$=(1+\tfrac{2}{3}\Omega^{0.6}+\tfrac{1}{5}\Omega^{1.2})\xi_r(s). \tag{3.8}$$

Note that for $\Omega=1$ we have $\xi_{\langle s\rangle}=(28/15)\xi_r$, which is quite similar to the rather crude estimate made in the Introduction for the increase of the squared density contrast for a homogeneous spherical perturbation. One can also compare this with the result obtained using Peebles' model for the distribution of peculiar velocities. Using Peebles' equation (76.9), with the streaming velocity given by equation (71.12), and integrating over directions, one obtains

$$\xi_{\langle s\rangle}(s)=(1+\tfrac{2}{3}\Omega^{0.6})\xi_r(s),$$

clearly different to our result (3.8)

The quantity $\xi_{\langle s\rangle}(s)$ has been estimated from the CfA survey by Davis & Peebles (1983), where the large solid volume of the survey permits the isotropic averaging indicated in equation (3.8). If we were to determine ξ_r by deprojection from

$$w_r(x)\equiv\int dz\,\xi_s(x,z),$$

where x is the component of s perpendicular to the line-of-sight and z is the parallel component, then by comparing with ξ_s we could determine Ω. Probably the simplest way to extract Ω is to form the quantity

$$w_s(x)\equiv\int dz\,\xi_{\langle s\rangle}[(x^2+z^2)^{1/2}],$$

and we then have

$$w_s(x)=(1+\tfrac{2}{3}\Omega^{0.6}+\tfrac{1}{5}\Omega^{1.2})w_r(x). \tag{3.9}$$

In order to carry out this procedure it is necessary to have sufficiently high signal-to-noise to be able to determine $\xi_s(\mathbf{s})$ in the linear regime where the amplitude is small. While surveys which have been performed to date have been rather limited in the volume of space covered, the situation should improve in the future for two reasons. First, one can expect the number of known redshifts to increase, and second, for the application considered here one can greatly improve the signal-to-noise ratio for a fixed number of redshifts by collecting redshifts only for a random sample of all galaxies and thereby sample a much larger volume of space (Kaiser 1986). Thus we

can reasonably hope that in the not too distant future the method described here should become a workable proposition.

For narrow cone surveys, and for objects seen in absorption against a distant QSO one is restricted to separations along the line-of-sight and so this test cannot be applied. We will now consider the problem of interpreting correlation functions obtained in this way.

3.3 LINE-OF-SIGHT CORRELATION FUNCTION

It would be very useful to be able to determine, from estimates of the correlation function restricted to the line-of-sight in s-space, which we shall denote by ξ_v, the true correlation function ξ_r, or equivalently the true power spectrum P_r. Unfortunately, knowledge of ξ_v alone is insufficient to uniquely determine P_r. Nevertheless, for any given P_r, one can determine ξ_v from equation (3.6), and one can hope that by experimenting with various forms for P_r, one can learn some of the general features of the relation between ξ_v and ξ_r, and thereby be able to draw some useful, if limited, inferences concerning P_r from observations of ξ_v.

Let us start with equation (3.6) then, with P_s given by equations (3.5). For $\mathbf{r}$ along the line-of-sight we can write

$$\xi_v(r)=4\pi \int_0^\infty dk\, k^2 P_r(k)\times\left[\sin kr\left\{\frac{1}{kr}+2\Omega^{0.6}\frac{[(kr)^2-2]}{(kr)^3}+\Omega^{1.2}\frac{[(kr)^4-12(kr)^2+24]}{(kr)^5}\right\}\right.$$
$$\left.+\cos kr\left\{\frac{4\Omega^{0.6}}{(kr)^2}+\Omega^{1.2}\frac{[4(kr)^2-24]}{(kr)^4}\right\}\right]. \tag{3.9}$$

In the limit that $\Omega\to0$, $\xi_v\to\xi_r$ as in equation (3.7). It is illustrative to consider the family of power law power spectra: $P_r(k)\propto k^n$, in which case the correlation function will also be a power law: $\xi_r\propto r^{-(n+3)}$. It is easy to see (by changing variables in (3.9) from k to $z\equiv kr$ that ξ_v will also be a power law with the same spectral index, but with a different amplitude, so we can write, in this case,

$$\xi_v=A(n)\xi_r. \tag{3.10}$$

Before we study the form of the function $A(n)$, it is helpful to consider a somewhat simpler example which will enable us to anticipate to some extent the form of the results. Consider a spherically symmetric density enhancement which has a power law profile $\Delta_r(\mathbf{r})=r^{-\gamma}$, with $\gamma>0$. Let us also assume, for simplicity, that $\Omega=1$, and restrict attention to the outer parts of the cluster where $\Delta_r\ll1$. The velocity field is then $\mathbf{v}(\mathbf{r})=-(\mathbf{r}/3)\Delta_{int}$, where Δ_{int} denotes the mean density contrast interior to r, and is given by $\Delta_{int}=3\Delta_r/(3-\gamma)$. It is relatively straightforward to show that the density contrast in s-space is given by

$$\Delta_s=\Delta_r-\frac{dU}{dr}=\Delta_r\left[\frac{4-\gamma(1+\mu^2)}{3-\gamma}\right]. \tag{3.11}$$

Various features of this result are worthy of note: first, the power law radial profile is preserved, but the density contrast in s-space has a strong quadrupolar component. Secondly, the density contrast in the transverse direction ($\mu=0$) is always enhanced, while the density contrast along the line-of-sight through the centre of the enhancement may or may not be enhanced depending on whether γ is less than or greater than unity, respectively. This result is quite easily understood: for $\Delta_r\propto r^{-1}$ the peculiar velocity is independent of radius so, along the central line-of-sight there is no shear, and so we see the true density contrast. For $\gamma<1$ the velocity shear is compressive, while for $\gamma>1$ the shear is rarefactive, and reduces the apparent density contrast. For $\gamma=2$ the shearing

just cancels the true density contrast and for steeper profiles there will exist regions in *s*-space where the density contrast is negative, even though Δ_r is everywhere positive. Thus the contours of density contrast will be grossly distorted when viewed in redshift space and the clusters will appear to be flattened along the line-of-sight. The analysis given here is restricted to the outer parts of the cluster where linear theory is valid. We will extend the analysis of the idealized power law cluster into the non-linear regime in Section 5.

Returning to the more interesting case of a stochastic density field with power law power spectrum $P_r(k)=k^n$, we can write

$$\xi_r=I_0 r^{-(n+3)},$$

$$\xi_v=(I_0+\Omega^{0.6}I_1+\Omega^{1.2}I_2)r^{-(n+3)},$$

where

$$I_0(n)=\int_0^\infty z^{2+n}\,dz\,\frac{\sin z}{z},$$

$$I_1(n)=\int_0^\infty z^{2+n}\,dz\left[(2z^2-4)\frac{\sin z}{z^3}+\frac{4\cos z}{z^2}\right],$$

$$I_2(n)=\int_0^\infty z^{2+n}\,dz\left[(z^4-12z^2+24)\frac{\sin z}{z^5}+(4z^2-24)\frac{\cos z}{z^4}\right].$$

These integrals can be evaluated numerically for any chosen value of n and the function $A(n)\equiv\xi_v/\xi_r$ is plotted in Fig. 1 for a range of n-values. In order to make the integrals converge it is necessary to introduce a smooth cut-off in the power spectrum at large wavenumber. For the results shown below we used a Gaussian, $P_r(k)=k^n\exp(-k^2/k_*^2)$. Provided that the cut-off is taken to be large, $k_*\gg1$, the results are independent of k_*.

The results are somewhat analogous to those obtained for the spherical cluster. For $n=-2$, $A=1$, so for this particular value of n, ξ_v gives a faithful representation of ξ_r. For steeper profiles,
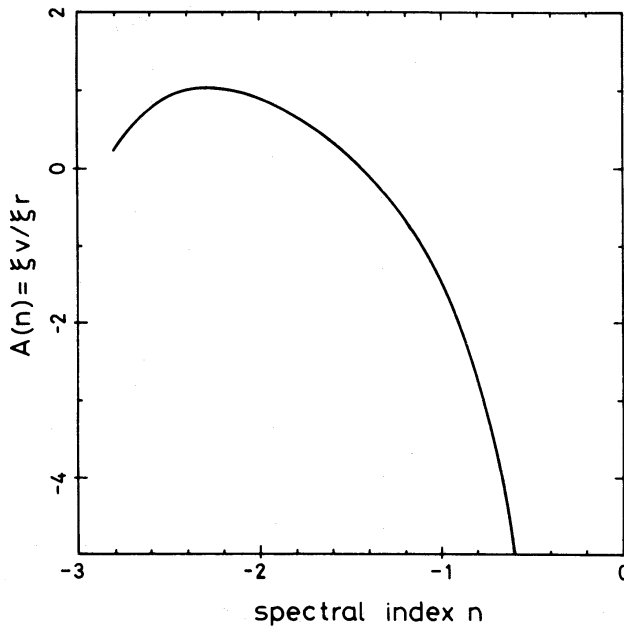

Figure 1. $A(n)$ is the ratio of ξ_v, the line-of-sight correlation function in redshift space, to ξ_r, the true correlation function, for a power law power spectrum $P(k)\propto k^n$. For values of the spectral index greater than about -1.4, ξ_v shows anticorrelation which can be very strong.

$n > -2$, ξ_v is smaller than ξ_r, due to negative shear. The cross-over point at which ξ_v vanishes is around $n \simeq -1.4$, and for more positive values of n one sees an apparent anticorrelation, which becomes very strong as n approaches 0.

It is probably unrealistic to assume a pure power law for $P_r(k)$. For instance, in the 'cold dark matter' scenario the slope of the power-spectrum is continuously varying. The special cases considered above do, however, allow one to draw some general conclusions concerning ξ_v. Consider the case in which the power spectrum consists of two power law regions which merge smoothly together in some way. The correlation function in r-space will then also asymptote to the appropriate slopes on small and large scales. The same will be true of ξ_v, but if the asymptotic values of n bracket the value $n \simeq -1.4$, ξ_v will be forced to change sign, and a spurious feature will emerge. In general then, one would expect features in ξ_r to be reflected as exaggerated features in ξ_v. Several concrete examples of the type of distortion that can arise are shown in Fig. 2, where
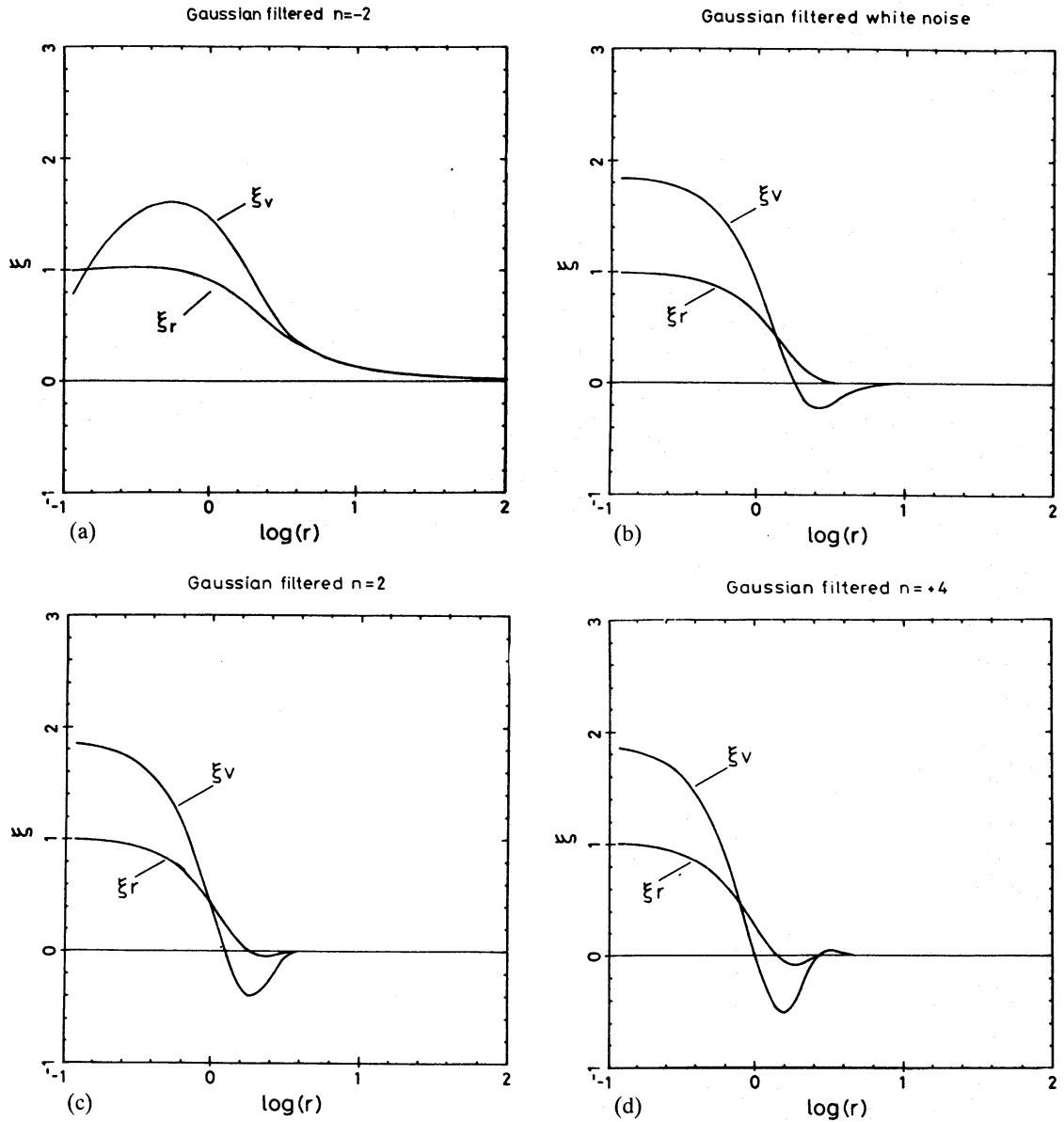

Figure 2. Line-of-sight correlation function in redshift space, ξ_v, and true correlation function, ξ_r, for various assumed spectra: (a) $P(k) \propto k^{-2} \exp(-k^2/2)$; (b) $P(k) \propto \exp(-k^2/2)$; (c) $P(k) \propto k^2 \exp(-k^2/2)$; (d) $P(k) \propto k^4 \exp(-k^2/2)$. In each case the amplitude has been chosen to give unit variance in r-space. Spurious anticorrelation is seen in many cases, and in all cases ξ_v is a very poor guide to ξ_r.

we have plotted ξ_r and ξ_v for various model power spectra. In all of these spectra a Gaussian 'low-pass filter' has been introduced in order to make the rms density fluctuation finite. We have normalized the variance to unity, but for any smaller variance one should simply reduce the correlation functions accordingly. As can be seen, there is a pronounced feature in ξ_v which has no counterpart in ξ_r.

This result is of some importance: if one assumes that the primordial spectrum of fluctuations asymptotes to the Zel'dovich spectrum at large scales, as for instance in the cold dark matter picture, then ξ_r should display an anticorrelation feature. This feature is predicted to be quite weak; it extends to very large radii but its volume integral is just large enough to cancel the positive contribution to $J_3 \equiv \int r^2 \xi_r \, dr$ at smaller radii. The examples shown in Fig. 2 show that much stronger features can arise in ξ_v for quite different reasons, and it will be practically impossible to learn much about the primordial spectrum from estimates of ξ_v alone. Certainly it would be unwise to interpret the anticorrelation feature suggested by the Durham analysis (Shanks *et al.* 1983) as evidence for a turnover to positive spectral index in the primordial power spectrum.

Another important implication of the foregoing concerns the clustering of absorption systems seen in QSO spectra. Lyman-α clouds appear to be rather weakly clustered in velocity space (Sargent *et al.* 1980; Webb 1986, in preparation). The analysis we have given above shows that distortions due to velocity shear are likely to be very important and must be taken into account in the interpretation of these data. As an example, note that one possible interpretation of the weak correlation seen is that the Lyman-α systems are in reality more strongly clustered, but that the power spectrum has a spectral index close to $n = -1.4$ on the relevant scale, so ξ_v is anomalously small. In any case, one can use the absence of any strong anticorrelation to put constraints on the possible values for n and Ω.

4 Determination of Ω from Virgo infall

In this section we consider the problem of determination of the density parameter from observation of the Virgo flow. This test requires two observations. First, one must determine the deceleration of the Hubble flow by the excess of matter in the local supercluster. This requires a determination of the distance to some sample of galaxies in the LSC, via a 'Tully–Fisher', or analogous relation, and to a sample of much more distant galaxies, say in Coma, which are assumed to be partaking of the uniform Hubble flow. If absolute luminosities are determined from the apparent luminosities using redshift as a distance measure, then the LSC galaxies will have an $L-\sigma$ relation which is offset with respect to that of the distant galaxies, and this offset is interpreted as the perturbation in the Hubble flow. The second datum is an estimate of the density enhancement of the LSC which can be obtained from a complete redshift survey. Combining these gives an estimate of the density parameter from

$$\frac{\Delta H}{H} = -\frac{f(\Omega)}{3} \frac{\Delta \varrho}{\varrho},$$

in the linear approximation, or from an analogous relation if non-linearity is important. The important assumptions here are (i) that the dynamics be reasonably well described by the spherical model, and (ii) that the enhancement of galaxies in the LSC faithfully reflects a true excess of mass.

Several groups have now estimated the perturbation to the Hubble flow using a variety of distance estimators. There is a broad concensus that the Hubble flow in the LSC is retarded by about 20 per cent. The density contrast has been estimated from the CfA survey by DH to be

$\Delta\varrho/\varrho \simeq 2$, but, as they note, the Virgo cluster lies quite near to the edge of this survey and so this introduces some uncertainty. They remarked that independent data on the extension of the Virgo cluster beyond the boundary of the CfA survey would suggest that their estimate of the density contrast is too high. The revised Shapley–Ames catalogue has much better sky coverage for this purpose and YST estimate that $\Delta\varrho/\varrho \simeq 3$ from these data, and thereby find $\Omega \simeq 0.05$, a value which would seem to firmly exclude the possibility that the Universe has closure density unless galaxies are more strongly concentrated in the LSC than the matter.

This particular observation is rather crucial: on smaller scales such as in individual galaxies, pairs, groups and clusters etc. the mass-to-light ratios determined increase with mass scale, and would seem to permit an asymptotic value $\sim 2000 \, h \, M_\odot/L_\odot$ corresponding to closure density. The result of YST suggests that on scales exceeding that of rich clusters this increasing trend stops, with obvious consequences for the global density parameter.

Various workers have recently attempted to check the validity of some of the assumptions that go into this calculation (Bushouse *et al.* 1985; Lee, Hoffman & Ftaclas 1986; Villumsen & Davis 1986) by comparison with the results obtained from similar analyses applied to cosmological *N*-body simulation. These studies allow one to quantify the magnitude of the errors which are likely to arise due to such factors as asphericity, 'random' motions associated with substructure, and the tidal influence of external matter. It should be mentioned, however, that some tests have been performed to see how important such factors are likely to be in the LAC itself. Sandage & Tammann (1975) find that the infall pattern is remarkably cold; they claim that random peculiar velocities within the general infall pattern can be no more than $\sim 50 \, \mathrm{km \, s^{-1}}$. Lilje, Yahil & Jones (1987) have determined the quadrupole distortion of the Hubble flow within the LSC; they find that the contribution of this tidal stretch to our radial velocity component relative to Virgo is small, so it would appear that such effects are not very important. One might also question the assumed universality of the 'Tully–Fisher' relation used to determine the distances to the galaxies. The statistical errors quoted for the fractional change in the Hubble ratio are on the order of a few per cent, and so it is clearly necessary to believe that any systematic differences between the galaxies in the LSC and those in the more distant reference clusters is no larger than this.

In this section, we shall address another problem: the effect of peculiar velocities on the estimate of $\Delta\varrho/\varrho$ by YST. To this end, we have constructed a very simple dynamical model to simulate this distortion. We have taken a power law density enhancement embedded in a flat universe, with the velocity field determined from the spherically symmetric, non-linear model. This model breaks down for the central region of the cluster where shell crossing must occur, but since only a small fraction of the mass of the LSC resides in this region this is not a serious problem. This model is specified by two quantities which we take to be the recession velocity of the centre of the perturbation relative to the observer, v_{LSC}, and the amount by which this departs from the unperturbed Hubble flow at this distance, i.e. the peculiar infall velocity, v_{pec}. We then populated this three-dimensional model with galaxies drawn from a Schechter-type luminosity function, and constructed from this a magnitude-limited sample. Projections of this simulated catalogue, with galactic latitude boundaries as in the RSA catalogue, are shown in Fig. 3(a) and (b). The values of the parameters were $v_{\mathrm{LSC}}=1150 \, \mathrm{km \, s^{-1}}$ and $v_{\mathrm{pec}}=350 \, \mathrm{km \, s^{-1}}$. The luminosity function adopted had a faint end slope of index $\alpha = -1.2$, and an amplitude in accord with that obtained from estimates of the luminosity function from deep samples (Efstathiou & Silk 1983). In order to reproduce an overall $N(z)$ like that observed, the magnitude limit was chosen such that an L^* galaxy will just enter the catalogue at a distance of $2500 \, \mathrm{km \, s^{-1}}$. Fig. 3(a) shows the distribution of galaxies in real space when projected on to a plane perpendicular to the plane of the 'galaxy' (the centre of the 'LSC' lies at the 'North Galactic Pole'). For the parameters chosen, the density excess interior to our radius is only 80 per cent, and this is reflected in the appearance
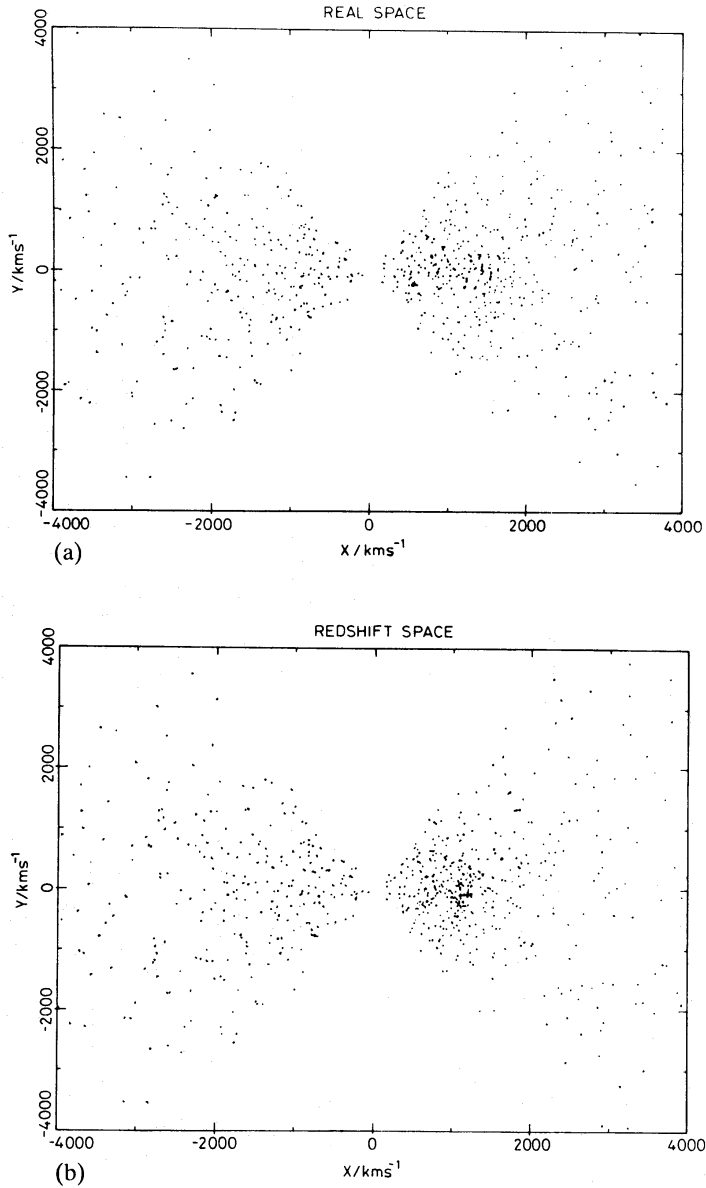
REAL SPACE

(a)

REDSHIFT SPACE

(b)

Figure 3. Simulation of a magnitude-limited redshift survey like the RSA survey. The points shown are 'galaxies' drawn from a realistic luminosity function. The observer is at the centre of the plots. The centre of the density concentration lies to the right of the observer, parameters are given in the text. (a) Shows the projection in real space on to a plane perpendicular to the observers galaxy. (b) Shows the analogous plot in redshift space. The density contrast interior to the sphere containing the observer is only 80 per cent, in accord with the modest appearance in *r*-space. The apparent overdensity in *s*-space is, however, much greater. The reader should compare this (3b) with the projections of the RSA catalogue shown in the plates accompanying the paper by YST.

of this plot. In Fig. 3(b) the same set of points is shown but now in redshift space. The density contrast is considerably enhanced, and the visual impression is quite similar to the projections of the RSA survey shown by YST.

In order to make a more quantitative comparison with the real survey we have calculated the density function for shells around us in a manner like that of YST, i.e. we define the density to be $\varrho_s \propto n_s/\phi$. This is shown, in Fig. 4 along with that calculated from the data (conveniently given in a table by YST). The acceleration is essentially just the integral of this function. The model and the data appear to be fairly similar, and so we conclude that, in so far as the parameters adopted are
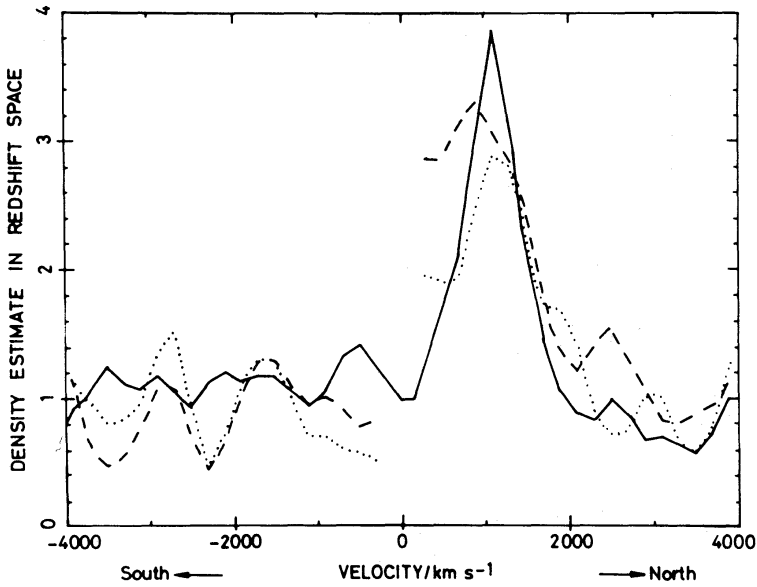
Figure 4. Density function in redshift space for northern (right half) and southern (left half) hemispheres. The solid line is for the model shown in Fig. 3. The dashed line is all the galaxies in the RSA and the dotted line is for the ellipticals and S0s (figures obtained from the table in YST). The model has a somewhat higher density in the south than the data (see text), otherwise the apparent amplitude is quite comparable.

allowed by the data, the redshift survey data are quite compatible with the Universe having closure density, and the overdensity of matter being the same as the overdensity of galaxies.

This result is in sharp discord with the conclusions of YST, and it is perhaps worth elaborating on the reasons for this discrepancy. First, our recession velocity from the centre of the supercluster was taken to be $1150 \, \mathrm{km \, s^{-1}}$, somewhat larger than the value of $1000 \, \mathrm{km \, s^{-1}}$ usually adopted for the Virgo cluster, and used by YST. We feel that this choice was not at all unreasonable. The value that is relevant for this calculation is the effective centre of the LSC, not the point which happens to have the greatest density, since most of the mass, and hence most of the source of our acceleration comes from the outer parts of the LSC. We first experimented with $v_{\mathrm{LSC}} = 1000 \, \mathrm{km \, s^{-1}}$, but found that the resulting density enhancement appeared to be too close to the observer. This turns out to be quite important, since the density contrast in both the model and the data is falling quite rapidly. Secondly, we allow for the distortion by peculiar velocities. In a more recent paper, Yahil (1981) claims that this correction is not very important, and, in any case, leads to a correction in the opposite sense from that which we have found. This is hard to reconcile with Fig. 3(a) and (b). Certainly the sign of this correction depends on the luminosity function adopted, and on other details. However, since few details of the calculation were given it is difficult to know to what one should ascribe the discrepancy. In any case, if the result is so sensitive to such parameters as the luminosity function, then any uncertainties in these estimates will feed through to the value of Ω derived. Thirdly, the baseline density adopted here was about 20 per cent higher than that adopted by YST. The reason for this is the independent evidence from the CfA survey that the southern galactic hemisphere region, which YST took to be at the background density, is in fact somewhat underpopulated with galaxies. As with the choice for v_{LSC}, while the data do not absolutely demand the values we have adopted, there does not seem to be any obvious conflict. Finally, we take the value of v_{pec} to be $350 \, \mathrm{km \, s^{-1}}$. It is possible to find estimates of this parameter which are lower by as much as a factor 2. Had we adopted such a value, the density contrast would have been considerably lower than observed. It is perhaps more reasonable to state this parameter in the form of the fractional perturbation to the Hubble flow,

since this is closer to what is actually measured. For the parameters chosen in the model illustrated we have $\Delta H/H$ is $350/(1150+350)\simeq23$ per cent.

We conclude then, that, from the reasonable likeness of the model to the data, one cannot exclude the joint hypothesis that the Universe has closure density and galaxies are clustered like the mass on the scale of the LSC. On the other hand, due to the highly idealized nature of the model, the considerable uncertainty in the data, and particularly the strong dependence of the derived density parameter on the infall velocity, we do not feel that a value of Ω considerably less than unity, $\Omega=0.2$ say, can be firmly excluded either.

The value of Ω obtained in this way, or, almost equivalently, the mass-to-light ratio of the LSC, has important implications for theories of galaxy formation, particularly those invoking 'biasing' mechanisms. If one appeals to the clustering statistics of high peaks (Bardeen *et al.* 1986) to account for the M/L variations, and reconcile these with the Universe having closure density, one finds that M/L should be quite a sensitive function of the density of the final system. Finding a mass-to-light ratio in the LSC as low as for rich clusters is an embarrassment for these models for two reasons. First, as stressed by Peebles (1986), it is hard to see how the presumably small density enhancement of the LSC at earlier times could have led to an enhancement of the efficiency of galaxy formation by the factor 5 or so required. Secondly, even if one could achieve this, one would then predict a much lower M/L for clusters than is observed. The result obtained here shows that the required bias, at least for the outer parts of the LSC, may be quite small, and it may be that only in the inner regions of the LSC is the mass-to-light ratio significantly lower than the closure value. The best way to resolve this question observationally is via the method described in Section 3, since this sidesteps the difficulties encountered when one attempts to estimate the density contrast in our neighbourhood.

5 Morphology of clusters and superclusters

In Section 2 we found that, at large separations where linear theory should provide a valid description, the clustering pattern, as measured by the correlation function for instance, should be strongly anisotropic. The sign of this anisotropy is an elongation of the power spectrum, P_s along the line-of-sight, corresponding to a compression of structures along the line-of-sight in s-space. In contrast to this, in the dense virialized parts of clusters, we find the familiar 'finger of God' elongation. These dense regions are highly non-linear, having density contrasts of a few hundred or so. It is of great interest to know what happens in the intermediate regime, i.e. for systems which are marginally non-linear.

Let us consider, for simplicity, the simple power law density enhancement for which we examined the outermost parts in Section 3. As we move in to smaller radii and larger density contrasts we eventually reach a point where the interior density contrast $\Delta_{int}\simeq4.5$. Particles on a shell at this radius are just turning around to fall back towards the cluster centre and so this spherical shell in r-space maps to a plane at constant z in s-space. Interior to this, successive shells will be inverted in s-space and, starting from a very flattened shape will become more and more elongated along the line-of-sight. We have taken a thin slice through such a cluster (omitting the central virialized portions) and the results are shown in Fig. 5(a) and (b), respectively. As can be clearly seen, a caustic surface has resulted; on this surface the density of matter is formally infinite, though the amount of matter at infinite density is formally zero; the density falling off inside the caustic surface inversely as the square-root of the distance. The density enhancement in the transverse direction is appreciable even outside the turnaround point where the actual caustic starts, and, at large radius this will match on to the butterfly-shaped density contours described in Section 3.
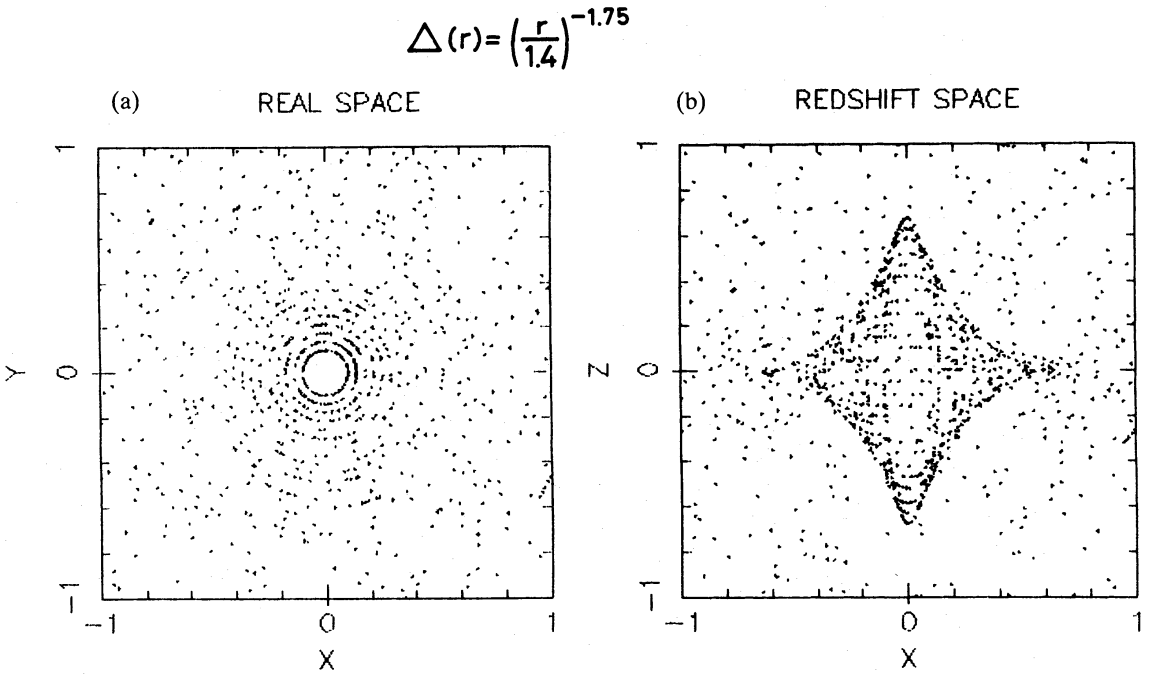
$$\triangle (r) = \left(\frac{r}{1.4} \right)^{-1.75}$$

(a)   REAL SPACE   (b)   REDSHIFT SPACE

Figure 5. Spherical cluster with power law density profile in *r*-space (a) and as it appears in redshift space (b). The points shown are those which lie in a thin equatorial slice through the cluster centre. Points in the central virialized portion have been omitted. Innermost points are falling into the cluster for the first time. The sampling density and separation between shells are such that individual shells can still be seen in *s*-space (*z*-coordinate is the redshift direction). The density contrast profile is $\Delta(r)=(r/1.4)^{-1.75}$. A caustic surface has resulted in *s*-space which, in three dimensions, has the form of two trumpet horns glued face to face. The caustic surface extends to the turnaround radius which lies at roughly twice the central 1D velocity dispersion, or about $20\,h^{-1}\,\mathrm{Mpc}$ for a cluster like Coma.

The caustic surface extends to the point at which the density contrast is $\simeq 4.5$. We can get the idea of the likely scale of such features around real rich clusters since we know from the virial theorem that, for a cluster with central velocity dispersion $1000\,\mathrm{km\,s^{-1}}$ say, the density is $\simeq 200\,\varrho_{\mathrm{crit}}$ at the Abell radius $r_{\mathrm{Abell}}=150\,\mathrm{km\,s^{-1}}$. Combining this with the estimate of the typical profile around a rich cluster which is given by the cluster–galaxy cross-correlation function $\xi_{\mathrm{cg}} \propto r^{-1.7}$ at large *r* (Seldner & Peebles 1977), we estimate the turnaround radius to be at around $1500\,\mathrm{km\,s^{-1}}$ (readers who wish to think in terms of physical distances will need to divide by their favourite value for the Hubble constant). To estimate this radius we have assumed that the profile of mass around a cluster is similar to the profile of the galaxies. The scale of regions turning around is quite impressive: compared with the 'finger of God' artefacts which contain only a very small fraction (~5 per cent) of all galaxies, we expect these transverse artefacts to contain roughly one order of magnitude more galaxies.

The cold spherical model is highly idealized, and it is important to consider how the results would change in a more realistic situation. It would be surprising indeed if real cluster profiles were highly spherically symmetric. In the more realistic case one would expect the caustic surfaces to be quite distorted. This would mean that the caustics would probably not be very visible in projection, in a solid volume survey like the CfA survey. They would, however, be expected to be just as prominent as those displayed here in a slice-like redshift survey and the inverse square root density run behind the caustic is a general feature, requiring only that the velocity field be sufficiently smooth, and of sufficient amplitude that the radial velocity should have turning points. Moreover, one would expect the characteristic scale of these transverse features to be similar to the estimate given above. More important for the visibility of these

caustics is the presence or absence of substructure. If the density field is clumpy on small scales, the peculiar velocities associated with this clumpiness will tend to smear out the caustics. The requirement for pronounced caustics is that the peculiar velocities on small scales should be much less than the scale of the caustics. The evidence of the smoothness of the LSC flow (Sandage & Tammann 1975) suggests that this condition is amply satisfied.

Thus we find that from a simple estimate of the turnaround radius, combined with the lack of very large peculiar velocities on small scales that there should be a strong tendency for galaxies to line up in smooth connected features; that these artefacts should match smoothly on to the 'fingers of God' like the 'trumpet horns' seen in Fig. 5(b); and that the features should be most prominent in slice-like redshift surveys, being less prominent in projection. It is easy to find examples of clusters which display the type of feature shown in Fig. 5(b). Perhaps the best example is in the study of the Perseus–Pisces region by Giovanelli & Haynes (1985) wherein some of the clusters are distinctly cross-like. Indeed, the whole complex studied by Giovannelli & Haynes lies at a roughly constant redshift, with some extremely narrow features in redshift space (see especially fig. 4 in Giovanelli *et al.* 1986) perhaps suggesting that here, in this region selected because of its great enhancement of galaxies and clusters seen on the sky, we have a very large region turning around.

Narrow, connected features are also seen in the slice-like survey of de Lapparent *et al.* (1986). They interpreted these as being shells from giant cosmological explosions. It is easy to see from Fig. 5(b) that with a few clusters scattered around in or near the slice surveyed that the caustics generated might give this impression if velocities are naively interpreted as distances. Generalizing from the highly symmetric example of Fig. 5(b), one can expect that underdense regions ('voids') would tend to be surrounded by sharply defined convex surfaces. One unrealistic feature of the model shown here is that there are no regions with density less than the mean density so one would expect the voids in the more realistic situation to be emptier than the low-density regions shown in the figure. Again, this seems to be quite compatible with the observations. Thus, the scale and morphology of the structures seen is in reasonable accord with what one would expect based on our crude estimate of the scale of regions turning around today.

The form of the spherical cluster as seen in redshift space can also shed some light on the falling velocity dispersion profile commonly seen in rich clusters such as Coma (Kent & Gunn 1982), and Perseus (Kent & Sargent 1983). These studies were confined to projected radii up to about $400–500 \, \text{km s}^{-1}$, or somewhat less than half of the central velocity dispersion. The caustic in Fig. 5(b) extends to a radius of about twice the central velocity dispersion, so we should compare the studies of Coma and Perseus with the inner parts of the model. In the spherical model it is considerably more difficult to follow the trajectories of the particles after shell crossing, and we have simply not plotted particles in the centre, which, assuming a central velocity dispersion of $100 \, \text{km s}^{-1}$ would correspond to a radius of about $200 \, \text{km s}^{-1}$. Were we to superimpose a virialized core, this would give a 'finger of God' that would sit inside the elongated caustic surface. Comparing with the azimuthally averaged velocity versus projected radius plots shown in the above quoted references we see that the velocity dispersion that one would infer falls by about the same amount as that observed. The observations have usually been interpreted in the framework of equilibrium models (see also Merritt 1987), with the hope of constraining the dynamical models and/or variations in mass-to-light ratios. The results obtained here suggest that, in so far as the real systems mimic the spherical model, such a model would be quite inappropriate, at radii more than a couple of hundred km s^{-1}, and what we are seeing in the outer parts of the clusters is essentially unequilibrated infall. Finally, it is worth noting that if this interpretation is correct, the distribution of velocities should be highly non-Gaussian and box-like. If we imagine a somewhat smeared-out version of the model, as one would expect due to departures from exact spherical symmetry, one would still expect the edges of the distribution in velocity space to be

fairly well defined. This is in accord with what is observed, where in Kent & Gunn's plot of the Coma cluster in velocity and projected radius for instance, their seems to be an unambigious distinction between members and non-members.

6 Discussion

In the analysis and models presented so far we have assumed that on the relevant scales, the galaxies 'fairly trace' the mass distribution. This assumption does not require that all of the mass be tied up in galaxies (we know from virial analyses of clusters of galaxies that there is a great deal of intergalactic material), but that in a region of space containing many galaxies, the number of galaxies gives an unbiased estimate of the amount of matter. We have seen that, if this assumption is valid, Ω can be determined from estimates of ξ_s via equation (3.9). It might be thought that, on sufficiently large-scales, the galaxy distribution must trace the mass. In one sense this is correct, in that if we count the number of galaxies N_g, and measure the mass, M, in some volume, then for large enough volumes N_g/M must tend to the global average value. However, the methods for determining Ω discussed here depend on the perturbation in N_g faithfully reflecting the mass perturbation, so we need $\Delta N_g/N_g = \Delta M/M$, and it is by no means certain that this condition is satisfied.

In 'biased' models for galaxy formation (see e.g. Bardeen *et al.* 1986, and references therein) this assumption would be violated. In such models, one appeals to modulation of the galaxy formation process by large-scale density fluctuations to cause variations in the mass-to-light ratio. In this way one can hope to reconcile the low M/L found for galaxy clusters with the Universe as a whole having closer density. Various mechanisms have been suggested to effect this biasing, but a common feature of these schemes is that they give rise to a linear modulation of galaxy formation by small-amplitude density fluctuations on very large scales. In particular, in models which invoke a threshold selection one finds that $\Delta N_g/N_g = (1+\alpha)\Delta M/M$, with α a constant determined by the threshold and time of formation of the galaxies. Once galaxy formation terminates, $\Delta M/M$ will continue to grow, and eventually the bias will become negligible. Thus, if galaxy formation occurred sufficiently early, while the galaxy distribution may have been strongly biased at that time, the present value of α will be very small, and the large-scale clustering will be essentially unbiased. If we invoke the threshold model, it turns out that, if we have sufficient biasing to account for the low M/L in rich clusters, then we should see significant biasing even on arbitrarily large scales (i.e. the present value of α should be close to unity). While this estimate of α is rather crude, the result is supported by the numerical simulations in which this threshold selection for 'galaxies' has been implemented.

Since the effect of this type of bias is simply to linearly enhance any large-scale clustering, this would be indistinguishable from an unbiased universe with a lower density parameter $\Omega_{\text{effective}} = (1+\alpha)^{-1/0.6} \simeq 0.3$. Thus, a test of such theories is provided by the method of Section 3: if we measure $\Omega \simeq 1$, we can rule out this model. In the framework of biased models the value of Ω derived from the dynamical methods discussed here tells us more about the galaxy formation process than the actual density parameter. If the threshold-biasing model is appropriate then the real Ω must be determined by other methods.

Biasing of the galaxy distribution in this way will also effect the distortions discussed in Section 5. If the large-scale structure is unbiased then regions with $\Delta N_g/N_g \simeq 4$ will be turning around today and suffering gross distortions in s-space. If the distribution is biased, and has $\alpha \simeq 1.0$, then the density contrast is much lower so these regions will still be expanding, and consequently any distortions will be much less pronounced. In the limiting case of very strong biasing, $\alpha \gg 1$, as might be applicable to rich clusters, the effective value of Ω will be very small and there would be effectively no distortion.

Acknowledgments

References

Bardeen, J. M., Bond, J. R., Kaiser, N. & Szalay, A., 1986. *Astrophys. J.,* **304,** 15.
Bushouse, H., Melott, A. L., Centrella, J. & Gallagher, J. S., 1985. *Mon. Not. R. astr. Soc.,* **217,** 7P.
Davis, M. & Huchra, J., 1982. *Astrophys. J.,* **254,** 437 (DH).
Davis, M. & Peebles, P. J. E., 1983. *Astrophys. J.,* **267,** 465.
de Lapparent, V., Geller, M. J. & Huchra, J. P., 1986. *Astrophys. J.,* **302,** L1.
Efstathiou, G. P. & Silk, J., 1983. *Fund Cos. Phys.,* **9,** 1.
Giovanelli, R. & Haynes, M. P., 1985. *Astr. J.,* **90,** 2445.
Giovanelli, R., Haynes, M. P. & Chincarini, G. L., 1986. *Astrophys. J.,* **300,** 77.
Kaiser, N., 1986. *Mon. Not. R. astr. Soc.,* **219,** 785.
Kent, S. M. & Gunn, J. E., 1982. *Astr. J.,* **87,** 945.
Kent, S. M. & Sargent, W. L. W., 1983. *Astr. J.,* **88,** 697.
Kirshner, R. P., Oemler, A. & Schechter, P. L., 1979. *Astr. J.,* **84,** 951.
Lee, H., Hoffman, Y. & Ftaclas, C., 1986. *Astrophys. J.,* **304,** L11.
Lilje, P. B., Yahil, A. & Jones, B. J. T., 1987. *Astrophys. J.,* **307,** 91.
Merritt, D., 1987. *Astrophys. J.,* **313,** 121.
Peebles, P. J. E., 1980. *The Large-Scale Structure of the Universe,* Princeton: Princeton University Press.
Peebles, P. J. E., 1986. *Nature,* **321,** 27.
Sandage, A. & Tammann, G. A., 1975. *Astrophys. J.,* **196,** 313.
Sargent, W. L. W., Young, P. J., Boksenberg, A. & Tytler, D., 1980. *Astrophys. J. Suppl.,* **42,** 41.
Seldner, M. & Peebles, P. J. E., 1977. *Astrophys. J.,* **215,** 703.
Shanks, T., Bean, A. J., Efstathiou, G., Ellis, R. S., Fong, R. & Peterson, B. A., 1983. *Astrophys. J.,* **274,** 529.
Villumsen, J. V. & Davis, M., 1986. *Astrophys. J.,* **308,** 499.
Yahil, A., 1981. *Tenth Texas Symp. Relativistic Astrophysics, Annals N.Y. Acad. Sci.*
Yahil, A., Sandage, A. & Tammann, G. A., 1980. *Astrophys. J.,* **242,** 448 (YST).